

# Large Vision-Language Model Alignment and Misalignment: A Survey Through the Lens of Explainability

Anonymous ACL submission

## Abstract

Large Vision-Language Models (LVLMs) have demonstrated remarkable capabilities in processing both visual and textual information. However, the critical challenge of alignment between visual and textual representations is not fully understood. This survey presents a comprehensive examination of alignment and misalignment in LVLMs through an explainability lens. We first examine the fundamentals of alignment, exploring its representational and behavioral aspects, training methodologies, and theoretical foundations. We then analyze misalignment phenomena across three semantic levels: object, attribute, and relational misalignment. Our investigation reveals that misalignment emerges from challenges at multiple levels: the data level, the model level, and the inference level. We provide a comprehensive review of existing mitigation strategies, categorizing them into parameter-frozen and parameter-tuning approaches. Finally, we outline promising future research directions, emphasizing the need for standardized evaluation protocols and in-depth explainability studies.

## 1 Introduction

Recent Large Vision-Language Models (LVLMs) have achieved significant progress in multimodal understanding. Models such as GPT-4V (OpenAI), Gemini (Team et al., 2023), LLaVA (Liu et al., 2024b), Claude-3.5-Sonnet (Anthropic, 2024), Qwen2-VL (Wang et al., 2024d), and LLaMa 3.2 (Dubey et al., 2024) demonstrate remarkable capabilities in tasks like image captioning and visual question answering, not only processing visual and textual information independently but also reasoning across these modalities. These advances are built upon two key foundations: large language models (LLMs) and vision encoders. LLMs such as GPT-3.5 (Brown, 2020), LLaMA (Touvron et al., 2023a), LLaMA 2 (Touvron et al., 2023b), and Qwen (Bai et al., 2023a) transformed natural

language processing, while visual understanding models like Vision Transformer (ViT) (Dosovitskiy et al., 2021) and vision-language models like CLIP (Radford et al., 2021) have advanced the ability to process visual information and create aligned visual-textual representations respectively.

The key challenge in developing effective LVLMs lies in achieving proper alignment between visual and textual representations (Liu et al., 2024a). The predominant approach involves using representation alignment techniques, where visual features from an image encoder and textual representations from an LLM are mapped into a shared embedding space, typically matching the LLM’s embedding dimensions (Jia et al., 2021; Yang et al., 2022; Shu et al., 2024). Once both modalities are mapped into this shared space, alignment can be achieved through various training objectives and architectural designs that encourage the model to understand and reason about cross-modal relationships. This method has gained popularity due to its straightforward approach and generalizability across different model architectures.

However, the current understanding of alignment mechanisms remains limited. A critical challenge lies in misalignment phenomena, which manifest in various forms. For instance, when shown an image of a green apple, the model might fail to recognize the apple altogether (object misalignment), incorrectly describe it as red (attribute misalignment), or generate incorrect relationships like “the apple is floating in the air” when it’s sitting on a table (relational misalignment). These misalignments lead to reliability issues (Zhang et al., 2024; Zhou et al., 2024; Zhao et al., 2024e), where models generate textual outputs that are inconsistent with the visual input. Understanding and addressing these misalignment issues is crucial for developing more reliable and trustworthy LVLMs, as they directly impact the models’ ability to generate accurate and consistent multimodal outputs.

In this survey, we present a structured framework for understanding and addressing alignment challenges in LVLMs from an explainability perspective. We first examine the fundamentals of alignment, including its representational and behavioral aspects, training procedures, and theoretical foundations. We then analyze misalignment phenomena across three semantic levels: object, attribute, and relational misalignment. Our investigation reveals that misalignment stems from challenges at the data level (e.g., quality and balance issues), model level (e.g., architectural limitations and ability gaps), and inference level (e.g., task discrepancies). We review existing mitigation strategies and outline future directions, emphasizing the need for standardized evaluation protocols and in-depth explainability studies.

## 2 Alignment of LVLMs

In this section, we examine alignment in LVLMs across four essential dimensions. First, we define the concept of alignment in LVLMs. Second, we detail the procedural stages through which alignment is achieved in practice. Third, we explore the theoretical foundations that make alignment possible between visual and textual modalities. Finally, we discuss methods for measuring and evaluating alignment in LVLMs in Appendix B.

### 2.1 What is Alignment?

In the context of LVLMs, let  $\mathcal{X}$  be the image space and  $\mathcal{T}$  be the text space. We define the alignment in two fundamental aspects: representational alignment and behavioral alignment.

- *Representational alignment* refers to the degree of correspondence between visual representations  $v \in \mathcal{V}$  and textual representations  $t \in \mathcal{T}$  within the model’s internal embedding space  $\mathcal{E}$ . When well-aligned, the visual features extracted from an image and the textual embeddings of its corresponding description occupy nearby regions in the shared latent space, exhibiting high semantic similarity  $d(v, t)$  where  $d$  is a similarity metric. This internal alignment enables the model to establish meaningful connections between visual and textual information at a fundamental level.
- *Behavioral alignment* refers to the model’s ability to generate accurate, factual, and consistent textual responses  $y \in \mathcal{Y}$  when processing image inputs  $x \in \mathcal{X}$ . A behaviorally aligned LVLM can reliably answer questions about visual content,

provide precise descriptions, and perform reasoning tasks without introducing errors or hallucinations. This external manifestation ensures that the model’s outputs faithfully reflect the actual content and relationships present in the images.

These two aspects of alignment are inherently connected. Strong representational alignment typically supports better behavioral alignment, as the model can more effectively leverage both visual and textual information to generate reliable outputs. Conversely, poor alignment in either aspect can lead to issues such as mismatched representations, inaccurate responses, or hallucinated content.

### 2.2 How is Alignment Achieved?

The development of alignment in LVLMs progresses through three major stages (see Figure 3 in Appendix), each is built upon its predecessor to achieve increasingly sophisticated cross-modal integration. Additionally, we present prominent real-world LVLM architectures in Appendix A.

**Stage 1: Training Visual Encoders.** The foundation of LVLM alignment begins with training visual encoders through contrastive learning, exemplified by models like CLIP (Radford et al., 2021). In this stage, the model learns to align visual and textual representations in a shared embedding space through a contrastive loss function. The process involves training on large-scale image-text pairs where matching pairs are pulled together in the embedding space while non-matching pairs are pushed apart. This leads to the development of robust visual representations that can meaningfully correspond to textual descriptions. Through this process, a visual encoder is created that can extract semantically meaningful features from images in a way that naturally aligns with language. This initial stage is crucial as it establishes the basic capability for cross-modal understanding, though the alignment is still relatively coarse-grained.

**Stage 2: Adapter Fine-tuning.** The second stage involves fine-tuning an adapter module that bridges the pre-trained visual encoder with the language model. This stage introduces lightweight adapter architectures, which typically consist of simple components such as linear layers, MLPs, or cross-attention layers that learn to translate between visual and language model embedding spaces. For example, cross-attention layers can feed image encoder representations into the language model, enabling the model to attend to relevant visual fea-

tures when generating text (Meta AI, 2024). A key characteristic of this approach is the preservation of the original capabilities of both the visual encoder and language model while learning to interface between them. During adapter training, while the visual encoder parameters may be updated, the language model parameters often remain frozen to maintain their original text capabilities. This intermediate stage is essential for establishing effective connections between modalities while preserving the specialized capabilities of each component.

**Stage 3: End-to-End Fine-tuning.** The final stage involves comprehensive fine-tuning of the entire system, including the visual encoder, adapter, and LLM components together. This comprehensive approach allows for deeper integration and more sophisticated alignment between all components. It enables the model to learn task-specific optimizations that require coordinated adjustments across all modules. Through this process, the model develops more advanced cross-modal understanding capabilities and facilitates the emergence of emergent behaviors that arise from the deep integration of visual and textual processing. This stage often results in the highest performance but requires careful balancing to avoid catastrophic forgetting or degradation of pre-existing capabilities.

### 2.3 Why is Alignment Possible?

Having established what alignment means and how it is implemented in LVLMs, a fundamental question arises: why is such alignment between vision and language modalities possible in the first place? The possibility of alignment between these modalities can be understood from both theoretical and algorithmic perspectives.

**Theoretical Perspective.** From a theoretical standpoint, visual and textual data are different projections of the same underlying reality. As Huh et al. argue in their Platonic Representation Hypothesis (Huh et al., 2024), all modalities are measurements of a real world that generates our observations. When humans create images or write text, they are encoding information about this same reality, though through different measurement processes. Although these modalities appear distinct on the surface, they fundamentally capture overlapping semantic information about the same world state. This shared origin in physical reality, combined with the fact that humans generate both types of data to describe their observations of the world,

provides the theoretical foundation for why these modalities can be meaningfully aligned in a common representation space.

**Algorithmic Perspective.** From an algorithmic perspective, although visual encoders and language models are initially trained separately on different modality-specific data, their learned representations inherently capture some similar semantic structures due to their training on human-generated data. Recent research has shown that these inherent similarities exist even before explicit alignment training (Maniparambil et al., 2024; Sharma et al., 2024; Neo et al., 2024). This natural compatibility serves as a starting point for more sophisticated alignment. The staged training process described in Section 2.2 then is built upon this inherent compatibility through systematic refinement: first using contrastive learning to organize embeddings in the shared latent space, then employing adapter fine-tuning to bridge between modalities while preserving their specialized capabilities, and finally conducting end-to-end training to enable deep integration across all components. Through this systematic combination of training stages and optimization objectives, the model gradually develops a robust alignment between the two modalities.

## 3 Misalignment of LVLMs

After introducing the alignment of LVLMs, we now examine a critical challenge facing these models: their tendency to generate outputs that diverge from the visual input. Despite significant advances in alignment techniques, LVLMs still frequently exhibit misalignment between their visual and textual inputs. In this section, we provide a comprehensive analysis of misalignment phenomena in LVLMs, beginning with a definition and taxonomy of different types of misalignment (see Figure 1), followed by an examination of their underlying causes.

### 3.1 Definition of Misalignment

Misalignment in LVLMs occurs when the model’s output semantically diverges from the visual content it is meant to describe. These discrepancies show in several key phenomena, impacting the overall performance of these models. In this paper, we categorize behavior-level misalignment phenomena in LVLM into three semantic levels  $\mathcal{S} = \{s_o, s_a, s_r\}$ : *object misalignment* ( $s_o$ ), *attribute misalignment* ( $s_a$ ), and *relation misalignment* ( $s_r$ ). Rather than using the term ‘hallucina-

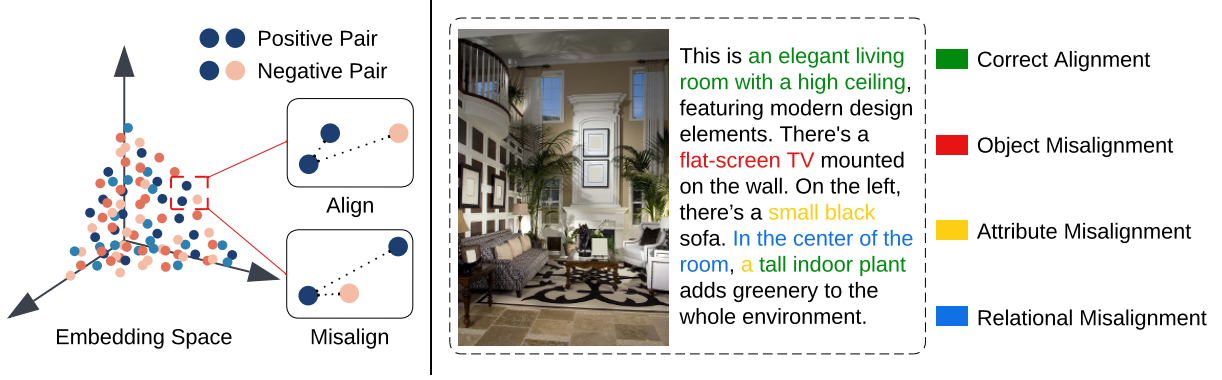


Figure 1: Illustration of representation-level and behavior-level alignment and misalignment in LVLMs. The **left** side shows **representation-level** phenomena in embedding space, where aligned visual-text pairs cluster together (positive pairs) while misaligned pairs are separated (negative pairs). The **right** side demonstrates **behavior-level** alignment and misalignment through a room description example, showing the spectrum from correct alignment (green) to various types of semantic misalignment: object misalignment (red), attribute misalignment (yellow), and relational misalignment (blue). These two levels are inherently connected, as the quality of representation alignment in the embedding space influences the model’s ability to generate semantically aligned outputs.

tion’ commonly found in the literature (Liu et al., 2024a), we adopt the term ‘misalignment’ to better characterize how these discrepancies emerge between visual and language representations.

- *Object Misalignment* ( $s_o$ ): This is one of the most widely recognized forms of misalignment (Liu et al., 2024a; Wang et al., 2023; Li et al., 2023b). It occurs when the model generates descriptions containing objects  $O'$  that differ from the actual objects  $O$  in the image, where  $O' \not\subseteq O$ . This represents the most coarse-grained level of misalignment, as it simply refers whether an object exists in the image or not. Due to its coarse-grained nature, object misalignment is relatively straightforward to detect and mitigate.
- *Attribute Misalignment* ( $s_a$ ): At a finer level, we identify attribute misalignment (Shang et al., 2024). This occurs when for an object  $o \in O$ , the model correctly identifies the object but generates incorrect attributes  $A' \neq A$ , where  $A$  represents the true attributes of  $o$ . Attribute misalignment typically involves adjectives or adverbs that describe properties of objects inaccurately. For example, when input an image of a green apple, the model might incorrectly describe the color of an apple as ‘red’ instead of ‘green’.
- *Relation Misalignment* ( $s_r$ ): This category involves the generation of incorrect or non-existent relationships  $R'$  between objects in an image (Wu et al., 2024b), where  $R'$  differs from the true relationships  $R$ . This misalignment manifests in two primary ways: spatial relationship errors and ac-

tion relationship errors. In spatial relationships, the model might incorrectly describe the relative positions of objects, such as saying ‘next to’ when the correct relation is ‘on top of’, or ‘inside’ when objects are merely ‘near’ each other. In action relationships, the model might generate semantically impossible interactions between objects, such as ‘he is walking a car’ instead of ‘he is driving a car’, or ‘the cat is reading a book’ instead of ‘the cat is sitting on a book’.

To better illustrate real-life examples of misalignment, we have selected four prominent LVLMs and provided their generated responses in Appendix D.

### 3.2 Reasons of Misalignment

Having identified the three semantic levels of misalignment phenomena, we now analyze their root causes across three fundamental levels: Dataset, Model, and Inference. The Dataset level examines how training data characteristics influence misalignment during learning. The Model level investigates how architectural decisions and training procedures affect alignment between modalities. The Inference level explores how the generation process can introduce misalignment even with well-aligned underlying representations.

#### 3.2.1 Dataset Level

Data quality and distribution patterns play crucial roles in contributing to misalignment between visual and language representations in LVLMs. Several key dataset factors can impede the model’s ability to form accurate associations between visual



inputs and textual descriptions, affecting both training effectiveness and inference performance. We list one factor below, for additional factors please refer to Appendix C.

- *Data imperfections*: This includes blurry images, vague or inaccurate captions, and mismatched image-caption pairs, which introduce significant challenges during training (Ouali et al., 2025; Shi et al., 2024). These quality issues manifest in various forms: images may suffer from poor resolution, inappropriate cropping, or visual artifacts; captions might contain grammatical errors, ambiguous descriptions, or factually incorrect information; and in some cases, the captions may describe content entirely unrelated to their paired images. These low-quality data points can distort the model’s ability to form precise mappings between modalities, leading to outputs that fail to accurately reflect the input image and potentially establishing incorrect associations that persist through the training process.

### 3.2.2 Model Level

Beyond data-level issues, the architectural design and training methodology of LVLMs significantly influence model alignment.

- *Ability Gap*: This independent pretraining process also creates an ability gap between the visual encoder and the LLM (Li et al., 2024c), where the LLM often demonstrates significantly greater capability than the visual encoder. Consequently, the LVLM tends to rely excessively on the LLM for predictions, resulting in imbalanced attention between visual and textual information (Chen et al., 2025; Min et al., 2024; Woo et al., 2024b).
- *Pretrain-finetuning Knowledge Gap*: After integrating the visual encoder and LLM into a unified LVLM, fine-tuning is typically performed to further enhance alignment and adapt the model to specific downstream tasks. However, this fine-tuning phase can introduce a pretraining-finetuning knowledge gap or conflict, where the general knowledge acquired during pretraining may clash with the specific requirements of the fine-tuning task (Zhou et al., 2024). Such conflicts can lead to knowledge forgetting, where the LVLM loses previously learned information while adapting to the new task (Zhou et al., 2023a; Huang et al., 2024b). Although knowledge forgetting might appear insignificant, it can have cascading effects. Each unit of knowledge

in the model’s embedding space is interconnected with lots of semantic relationships. Forgetting even a single piece of knowledge can disrupt these relational connections, undermining the integrity of the embedding space. This disruption causes a broader misalignment within the LVLM.

- *Knowledge Conflict*: A significant challenge arises from knowledge conflicts between the visual knowledge of image and parametric knowledge of LLM. These conflicts emerge when the visual encoder’s direct perception of image content contradicts the prior knowledge embedded in the LLM’s parameters during pre-training (Zhu et al., 2024b; Ghosh et al., 2024). For example, when an image contains a green tomato, the visual encoder accurately detects its color, but the LLM may resist this information since it has been predominantly trained on texts describing ripe, red tomatoes. This misalignment between observed visual evidence and learned textual priors can manifest in various ways: the model might incorrectly describe the tomato as red despite clear visual evidence, generate hesitant or self-contradicting descriptions, or attempt to rationalize the discrepancy by making unwarranted assumptions about the tomato’s ripeness stage.

### 3.2.3 Inference Level

Misalignment can also occur during the inference stage due to *task discrepancy*. This discrepancy fundamentally represents an out-of-distribution (OOD) generalization problem, as users often pose questions or request tasks that deviate from the distribution of examples seen during training. Even when a LVLM has been trained on a large and diverse dataset, it may encounter novel combinations of visual and textual elements or be asked to perform tasks in ways that differ subtly but significantly from its training examples. This OOD challenge manifests in several ways. First, the training data used for pre-training or fine-tuning the model may not fully align with the specific tasks it is later expected to perform (Zhang et al., 2024). For example, a model trained primarily on image captioning data might struggle when asked to answer specific questions about spatial relationships or perform detailed visual reasoning tasks. Second, users may phrase requests in ways that differ from the instruction patterns seen during training, leading to potential misinterpretation of the task requirements. Third, the visual inputs during inference may contain novel object configurations

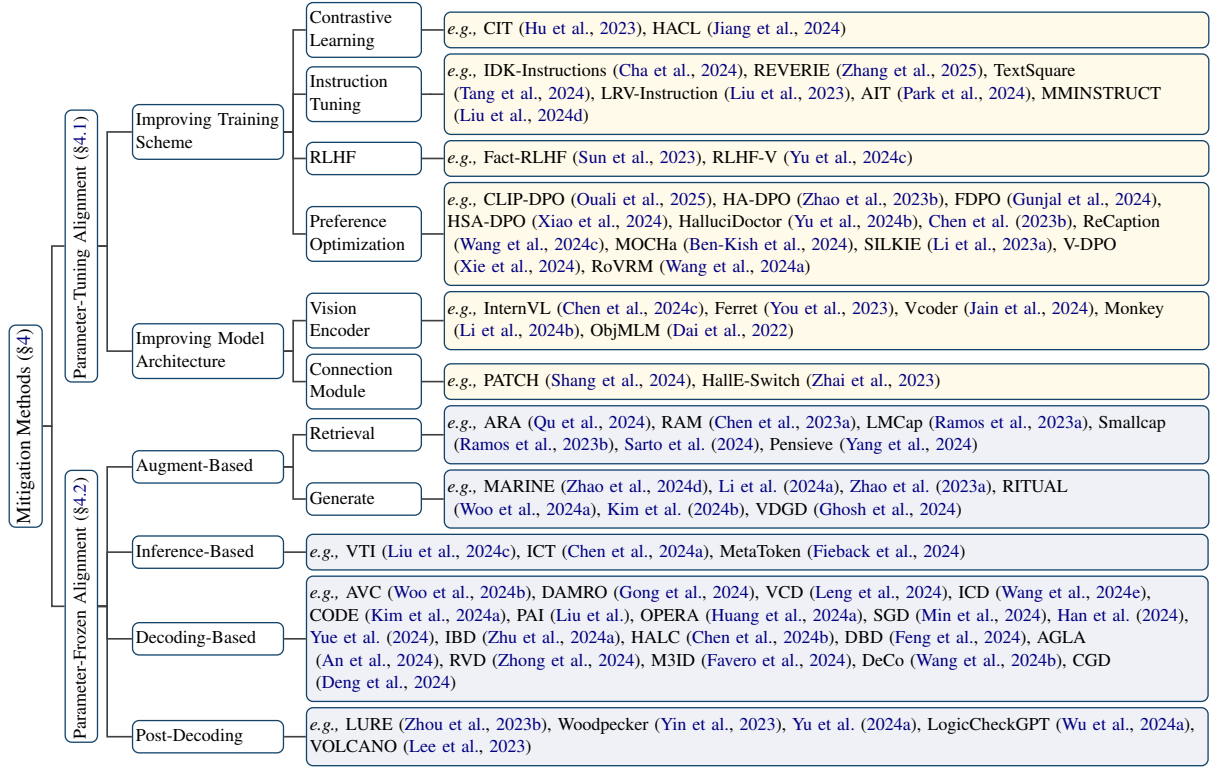


Figure 2: Taxonomy of Misalignment Mitigation Methods for LVLMs, including *Parameter-Tuning Alignment* and *Parameter-Frozen Alignment*.

or scene compositions not well-represented in the training data. These distribution shifts can create misalignment in LVLMs as the model struggles to adapt to new and distinct tasks that require different interpretations of visual and textual information.

## 4 Mitigation Methods

Building upon our analysis of misalignment causes in LVLMs, we now examine strategies for mitigating these challenges (see Figure 2). These mitigation approaches can be categorized into two groups: parameter-tuning alignment methods and parameter-frozen alignment methods. Parameter-tuning alignment involves modifying specific components within the LVLM architecture to reduce misalignment through targeted parameter updates. In contrast, parameter-frozen alignment methods address misalignment while maintaining the LVLM’s original parameters unchanged, offering solutions that preserve the model’s structure while improving its cross-modal alignment capabilities. We have conducted experiments comparing the performance and computational cost of several mitigation methods (see Appendix E for details).

### 4.1 Parameter Tuning Alignment

Parameter-tuning alignment focuses on mitigating misalignment by refining the training scheme or

enhancing the architecture itself.

**Improving Training Scheme.** Parameter-tuning methods that improve the training scheme often address misalignment broadly as a data-level issue or as a general visual-textual misalignment (Ouali et al., 2025; Jiang et al., 2024). This understanding leads to a straightforward objective, which is reducing the modality gap between visual and textual representations. This can often be achieved by improving the dataset quality or optimizing training techniques. One common approach is contrastive learning, exemplified by methods such as CIT (Hu et al., 2023) and HACL (Jiang et al., 2024). These techniques involve using a third model to generate positive and negative data pairs. The LVLM is then trained to bring the representations of positive pairs closer together while pushing negative pairs apart in the embedding space. Another widely adopted strategy is instruction tuning, as seen in LRV-Instruction (Liu et al., 2023) and TextSquare (Tang et al., 2024). Similarly, these approaches rely on a third model to generate instructional data, which is subsequently used to train the LVLM effectively. However, these approaches often lack robust quality assurance mechanisms to verify the accuracy or relevance of the generated data, introducing potential risks. Alternatively, Reinforcement Learn-

ing from Human Feedback (RLHF) employs human feedback to train a reward model, ensuring that the generated data aligns with human preferences (Sun et al., 2023; Yu et al., 2024c). While RLHF guarantees high-quality training data, it comes at a significant cost. To address this, some methods leverage preference optimization, wherein multiple responses are generated for the same input image, ranked or scored by a third model, and categorized into positive and negative pairs (Ouali et al., 2025; Zhao et al., 2023b; Gunjal et al., 2024). The model is then fine-tuned on this curated dataset. Although these methods can significantly improve the model, they are often constrained by either high resource requirements (as in RLHF) or the uncertain quality of generated data (as in contrastive learning and instruction tuning) or rerank model (as in preference optimization). This highlights the ongoing need for large, diverse, and high-quality datasets to effectively address data-level misalignment.

**Improving Model Architecture.** Methods that improve the model architecture often involve a deep understanding of the root causes of misalignment, allowing researchers to pinpoint deficiencies within specific components of the LVLM. Typical LVLM architectures consist of three main components: the visual encoder, the adapter module, and the LLM (Liu et al., 2024a; Bai et al., 2024). Most architecture-focused approaches concentrate on enhancing the visual encoder or the adapter module, with relatively few addressing improvements to the LLM itself. This aligns with our earlier model-level claim of the model ability gap, where the LLM often outperforms the visual encoder. Blindly enhancing the LLM could exacerbate this gap, potentially worsening the misalignment issue. To reduce this ability gap, some studies scale up the visual encoder by increasing its parameter size (Chen et al., 2024c). Others introduce additional components to the visual encoder to improve its capabilities without necessarily scaling up its size (You et al., 2023; Jain et al., 2024; Li et al., 2024b). In addition to the visual encoder, many methods focus on improving the adapter module, which serves as the critical bridge between the visual and textual modalities. Enhancements to the adapter module often involve adding intermediary layers or mechanisms to better align the visual encoder’s outputs with the LLM’s input requirements. For example, PATCH (Shang et al., 2024) employs trainable virtual tokens to enhance the projection layer, improving cross-modal

alignment. Similarly, Halle-Switch (Zhai et al., 2023) introduces a dynamic mechanism that adjusts the flow of information between the visual encoder and the LLM based on input complexity. By addressing these architectural components, parameter-tuning methods aim to reduce the modality gap and improve the alignment between visual and textual representations, ultimately enhancing the LVLM’s performance across tasks.

## 4.2 Parameter Frozen Alignment

Parameter-frozen alignment methods have gained increasing popularity due to their significant practical advantages. These training-free approaches are highly modular and easy to implement, allowing them to be readily integrated into existing systems without requiring costly retraining or fine-tuning processes. This makes them particularly attractive for real-world applications where computational resources may be limited. We categorize these parameter-frozen methods into four types based on where they intervene in the LVLM processing pipeline: Augment-based mitigation, augmenting the LVLM by incorporating external knowledge; inference-based mitigation, operating in the model’s latent space during intermediate processing; decoding-based mitigation, which guides the text generation process; and post-decoding mitigation, which refines the final outputs.

**Augment-based Methods.** As analyzed in Section 3, insufficient input of image information is one of the primary causes of misalignment, leading to poor visual understanding. To address this, retrieval-augmented generation (RAG) methods have been adapted to dynamically integrate external knowledge into LVLMs through retrieved results (Qu et al., 2024; Chen et al., 2023a; Ramos et al., 2023a,b; Sarto et al., 2024; Yang et al., 2024). By reranking the similarity of image-text pairs, RAG approaches provide more visual context and guidance to the model. Similarly, other methods rely on generating approach to enrich the input with additional information. For instance, Zhao et al. (2024d), Li et al. (2024a), and Zhao et al. (2023a) propose integrating an auxiliary model to generate relevant information based on the image. Alternatively, methods such as RITUAL (Woo et al., 2024a) bypass the need for external models. It enhances the model’s exposure to diverse visual contexts by applying random transformations to input images. Additionally, approaches like (Kim et al.,



2024b; Ghosh et al., 2024) employ self-generated textual descriptions appended to the input prompt, ensuring the model has sufficient knowledge to answer questions accurately.

**Inference-based Methods.** Some methods operate in the model’s latent space during the inference process, prior to decoding, by intervening in both visual and textual representations to improve alignment. For instance, Visual and Textual Intervention (VTI) (Liu et al., 2024c) pre-computes intervention directions using a small set of examples and applies them during inference to enhance feature stability and vision-text alignment, without requiring additional training. Similarly, Image-Object Cross-Level Trusted Intervention (ICT) (Chen et al., 2024a) introduces a lightweight mechanism that intervenes in the model’s attention at both image and object levels, applying targeted activation shifts to selected attention heads. Since they operate directly on the model’s internal representations, they can make precise adjustments to improve alignment without disrupting the model’s broader language understanding capabilities. This makes inference-based methods effective at reducing misalignment while preserving the model’s ability to generate contextually appropriate responses.

**Decoding-based Methods.** Another common approach to mitigating misalignment involves modifying the decoding process. These methods often target issues of imbalanced attention. However, the imbalance attention between what still remain debated. Some researchers argue that the model over-focuses on irrelevant image tokens, such as background elements or unimportant details (Woo et al., 2024b; Gong et al., 2024). However, the prevailing view is that the model prioritizes textual tokens over visual ones, neglecting critical visual information (Leng et al., 2024; Wang et al., 2024e; Kim et al., 2024a; Liu et al.). Despite these differences in interpretation, most decoding-based methods use contrastive decoding to rebalance attention between modalities, typically by reducing attention to textual tokens while enhancing focus on visual tokens. This approach, however, contrasts with inference-based methods, which avoid reducing attention to textual information and instead preserve the model’s overall language understanding. Another interesting observation is that, while decoding-based methods typically lead to similar approaches, they can sometimes result in divergent strategies. For instance, OPERA (Huang

et al., 2024a) hypothesizes that the model over-relies on summary tokens, instead of focusing visual tokens. However, text summarization is SGD’s solution (Min et al., 2024) to misalignment. It uses summarization to shorten textual context and helps model shift focus toward visual information. This divergence underscores how subtle differences in understanding misalignment’s root causes can lead to contradicted methodologies.

**Post-decoding Methods.** Lastly, post-decoding approaches present broader hypotheses about misalignment causes, tackling issues ranging from data-level biases to model-level deficiencies. Methods such as LURE (Zhou et al., 2023b) and Woodpecker (Yin et al., 2023) exemplify this category. LURE focuses on addressing object hallucinations by revising the generated text, identifying hallucinatory content, and reconstructing less biased outputs. Woodpecker employs a five stages validation mechanism to extract and correct inconsistencies in the generated response. Despite their specific details, these methods converge on a shared strategy, which involves modifying the model’s outputs after decoding without altering parameters or architecture, making them easily adaptable to various LVLMS. This flexibility lies in their goal-oriented nature, as they directly target specific misalignment phenomena.

## 5 Conclusions

In this paper, we systematically survey alignment and misalignment in LVLMS through an explainability lens. We show that achieving proper alignment involves complex interactions between data quality, model architecture, and inference procedures. We categorize misalignment into object, attribute, and relational levels, providing a clear framework to understand these challenges and develop targeted solutions. Our review of mitigation strategies highlights approaches ranging from computationally intensive parameter-tuning methods to practical parameter-frozen solutions, each with trade-offs in effectiveness and feasibility. Lastly, we outline key future directions for building robust vision-language systems (see Appendix F), including development of standardized benchmarks, deeper investigation into explainability approaches to reveal internal alignment mechanisms, and architectural innovations to address fundamental limitations in current designs.



## Limitations

While this paper provides a comprehensive survey of alignment and misalignment in LVLMs, we acknowledge there are several limitations. Currently, the scope of this survey is limited to the alignment between vision and language modalities. However, real-world applications often require the integration of multiple modalities, such as audio, video, or sensor data. We plan to expand the scope to explore the challenges and alignment techniques in such complex multi-modal settings, including investigating alignment mechanisms in architectures that incorporate three or more modalities, developing new evaluation metrics for multi-modal alignment, and studying the interactions between different modalities in integrated systems.

## References

Wenbin An, Feng Tian, Sicong Leng, Jiahao Nie, Haonan Lin, QianYing Wang, Guang Dai, Ping Chen, and Shijian Lu. 2024. Agla: Mitigating object hallucinations in large vision-language models with assembly of global and local attention. *arXiv preprint arXiv:2406.12718*.

Anthropic. 2024. [Claude 3.5 sonnet](#).

Jinze Bai, Shuai Bai, Yunfei Chu, Zeyu Cui, Kai Dang, Xiaodong Deng, Yang Fan, Wenbin Ge, Yu Han, Fei Huang, et al. 2023a. Qwen technical report. *arXiv preprint arXiv:2309.16609*.

Jinze Bai, Shuai Bai, Shusheng Yang, Shijie Wang, Sinan Tan, Peng Wang, Junyang Lin, Chang Zhou, and Jingren Zhou. 2023b. Qwen-vl: A versatile vision-language model for understanding, localization, text reading, and beyond. *arXiv preprint arXiv:2308.12966*.

Ze Chen Bai, Pichao Wang, Tianjun Xiao, Tong He, Zongbo Han, Zheng Zhang, and Mike Zheng Shou. 2024. Hallucination of multimodal large language models: A survey. *arXiv preprint arXiv:2404.18930*.

Assaf Ben-Kish, Moran Yanuka, Morris Alper, Raja Giryes, and Hadar Averbuch-Elor. 2024. Mitigating open-vocabulary caption hallucinations. In *Proceedings of the 2024 Conference on Empirical Methods in Natural Language Processing*, pages 22680–22698.

Tom B Brown. 2020. Language models are few-shot learners. *arXiv preprint arXiv:2005.14165*.

Jaeseok Byun, Dohoon Kim, and Taesup Moon. 2024. Mafa: Managing false negatives for vision-language pre-training. In *Proceedings of the IEEE/CVF Conference on Computer Vision and Pattern Recognition*, pages 27314–27324.

Sunguk Cha, Jusung Lee, Younghyun Lee, and Cheoljong Yang. 2024. Visually dehallucinative instruction generation. In *ICASSP 2024-2024 IEEE International Conference on Acoustics, Speech and Signal Processing (ICASSP)*, pages 5510–5514. IEEE.

Jingwen Chen, Yingwei Pan, Yehao Li, Ting Yao, Hongyang Chao, and Tao Mei. 2023a. Retrieval augmented convolutional encoder-decoder networks for video captioning. *ACM Transactions on Multimedia Computing, Communications and Applications*, 19(1s):1–24.

Junzhe Chen, Tianshu Zhang, Shiyu Huang, Yuwei Niu, Linfeng Zhang, Lijie Wen, and Xuming Hu. 2024a. Ict: Image-object cross-level trusted intervention for mitigating object hallucination in large vision-language models. *arXiv preprint arXiv:2411.15268*.

Liang Chen, Haozhe Zhao, Tianyu Liu, Shuai Bai, Junyang Lin, Chang Zhou, and Baobao Chang. 2025. An image is worth 1/2 tokens after layer 2: Plug-and-play inference acceleration for large vision-language models. In *European Conference on Computer Vision*, pages 19–35. Springer.

Zhaorun Chen, Zhuokai Zhao, Hongyin Luo, Huaxiu Yao, Bo Li, and Jiawei Zhou. 2024b. Halc: Object hallucination reduction via adaptive focal-contrast decoding. *arXiv preprint arXiv:2403.00425*.

Zhe Chen, Jiannan Wu, Wenhai Wang, Weijie Su, Guo Chen, Sen Xing, Muyan Zhong, Qinglong Zhang, Xizhou Zhu, Lewei Lu, et al. 2024c. Internvl: Scaling up vision foundation models and aligning for generic visual-linguistic tasks. In *Proceedings of the IEEE/CVF Conference on Computer Vision and Pattern Recognition*, pages 24185–24198.

Zhiyang Chen, Yousong Zhu, Yufei Zhan, Zhaowen Li, Chaoyang Zhao, Jinqiao Wang, and Ming Tang. 2023b. Mitigating hallucination in visual language models with visual supervision. *arXiv preprint arXiv:2311.16479*.

Wenliang Dai, Zihan Liu, Ziwei Ji, Dan Su, and Pascale Fung. 2022. Plausible may not be faithful: Probing object hallucination in vision-language pre-training. *arXiv preprint arXiv:2210.07688*.

Ailin Deng, Zhirui Chen, and Bryan Hooi. 2024. Seeing is believing: Mitigating hallucination in large vision-language models via clip-guided decoding. *arXiv preprint arXiv:2402.15300*.

Wangyuan Ding and Nanne Van Noord. Imp: Benchmarking image polysemy in vision-language models.

Alexey Dosovitskiy, Lucas Beyer, Alexander Kolesnikov, Dirk Weissenborn, Xiaohua Zhai, Thomas Unterthiner, Mostafa Dehghani, Matthias Minderer, Georg Heigold, Sylvain Gelly, Jakob Uszkoreit, and Neil Houlsby. 2021. An image is worth 16x16 words: Transformers for image recognition at scale. In *International Conference on Learning Representations (ICLR)*.

805	Abhimanyu Dubey, Abhinav Jauhri, Abhinav Pandey,	Wenke Huang, Jian Liang, Zekun Shi, Didi Zhu,	861
806	Abhishek Kadian, Ahmad Al-Dahle, Aiesha Letman,	Guancheng Wan, He Li, Bo Du, Dacheng Tao, and	862
807	Akhil Mathur, Alan Schelten, Amy Yang, Angela	Mang Ye. 2024b. Learn from downstream and be	863
808	Fan, et al. 2024. The llama 3 herd of models. <i>arXiv</i>	yourself in multimodal large language model fine-	864
809	<i>preprint arXiv:2407.21783</i> .	tuning. <i>arXiv preprint arXiv:2411.10928</i> .	865
810	Alessandro Favero, Luca Zancato, Matthew Trager, Sid-	Minyoung Huh, Brian Cheung, Tongzhou Wang, and	866
811	dharth Choudhary, Pramuditha Perera, Alessandro	Phillip Isola. 2024. The platonic representation hy-	867
812	Achille, Ashwin Swaminathan, and Stefano Soatto.	pothesis. <i>The International Conference on Machine</i>	868
813	2024. Multi-modal hallucination control by vi-	<i>Learning (ICML)</i> .	869
814	sual information grounding. In <i>Proceedings of the</i>	Fushuo Huo, Wenchao Xu, Zhong Zhang, Haozhao	870
815	<i>IEEE/CVF Conference on Computer Vision and Pat-</i>	Wang, Zhicheng Chen, and Peilin Zhao. 2024. Self-	871
816	<i>tern Recognition</i> , pages 14303–14312.	introspective decoding: Alleviating hallucinations	872
817	Mingqian Feng, Yunlong Tang, Zeliang Zhang, and	for large vision-language models. <i>arXiv preprint</i>	873
818	Chenliang Xu. 2024. Do more details always intro-	<i>arXiv:2408.02032</i> .	874
819	duce more hallucinations in lvlm-based image cap-	Jitesh Jain, Jianwei Yang, and Humphrey Shi. 2024.	875
820	tioning? <i>arXiv preprint arXiv:2406.12663</i> .	Vcoder: Versatile vision encoders for multimodal	876
821	Laura Fieback, Jakob Spiegelberg, and Hanno	large language models. In <i>Proceedings of the</i>	877
822	Gottschalk. 2024. Metatoken: Detecting halluci-	<i>IEEE/CVF Conference on Computer Vision and Pat-</i>	878
823	nation in image descriptions by meta classification.	<i>tern Recognition</i> , pages 27992–28002.	879
824	<i>arXiv preprint arXiv:2405.19186</i> .	Chao Jia, Yinfei Yang, Ye Xia, Yi-Ting Chen, Zarana	880
825	Chaoyou Fu, Peixian Chen, Yunhang Shen, Yulei Qin,	Parekh, Hieu Pham, Quoc Le, Yun-Hsuan Sung, Zhen	881
826	Mengdan Zhang, Xu Lin, Jinrui Yang, Xiawu Zheng,	Li, and Tom Duerig. 2021. Scaling up visual and	882
827	Ke Li, Xing Sun, et al. 2023. Mme: A comprehensive	vision-language representation learning with noisy	883
828	evaluation benchmark for multimodal large language	text supervision. In <i>International conference on ma-</i>	884
829	models. <i>arXiv preprint arXiv:2306.13394</i> .	<i>chine learning</i> , pages 4904–4916. PMLR.	885
830	Sreyan Ghosh, Chandra Kiran Reddy Evuru, Sonal Ku-	Chaoya Jiang, Haiyang Xu, Mengfan Dong, Jiaxing	886
831	mar, Utkarsh Tyagi, Oriol Nieto, Zeyu Jin, and Di-	Chen, Wei Ye, Ming Yan, Qinghao Ye, Ji Zhang,	887
832	nesh Manocha. 2024. Visual description grounding	Fei Huang, and Shikun Zhang. 2024. Hallucination	888
833	reduces hallucinations and boosts reasoning in lvlms.	augmented contrastive learning for multimodal large	889
834	<i>arXiv preprint arXiv:2405.15683</i> .	language model. In <i>Proceedings of the IEEE/CVF</i>	890
835	Xuan Gong, Tianshi Ming, Xinpeng Wang, and Zhihua	<i>Conference on Computer Vision and Pattern Recog-</i>	891
836	Wei. 2024. Damro: Dive into the attention mecha-	<i>nition</i> , pages 27036–27046.	892
837	nism of lvlm to reduce object hallucination. <i>arXiv</i>	Junho Kim, Hyunjun Kim, Yeonju Kim, and Yong Man	893
838	<i>preprint arXiv:2410.04514</i> .	Ro. 2024a. Code: Contrasting self-generated descrip-	894
839	Anisha Gunjal, Jihan Yin, and Erhan Bas. 2024. De-	tion to combat hallucination in large multi-modal	895
840	tecting and preventing hallucinations in large vision	models. <i>arXiv preprint arXiv:2406.01920</i> .	896
841	language models. In <i>Proceedings of the AAAI Con-</i>	Junho Kim, Kim Yeonju, and Yong Man Ro. 2024b.	897
842	<i>ference on Artificial Intelligence</i> , volume 38, pages	What if...?: Thinking counterfactual keywords helps	898
843	18135–18143.	to mitigate hallucination in large multi-modal models.	899
844	Zongbo Han, Zechen Bai, Haiyang Mei, Qianli Xu,	In <i>Findings of the Association for Computational</i>	900
845	Changqing Zhang, and Mike Zheng Shou. 2024.	<i>Linguistics: EMNLP 2024</i> , pages 10672–10689.	901
846	Skip\n: A simple method to reduce hallucination	Seongyun Lee, Sue Hyun Park, Yongrae Jo, and Min-	902
847	in large vision-language models. <i>arXiv preprint</i>	joon Seo. 2023. Volcano: mitigating multimodal	903
848	<i>arXiv:2402.01345</i> .	hallucination through self-feedback guided revision.	904
849	Hongyu Hu, Jiyuan Zhang, Minyi Zhao, and Zhenbang	<i>arXiv preprint arXiv:2311.07362</i> .	905
850	Sun. 2023. Ciem: Contrastive instruction evaluation	Sicong Leng, Hang Zhang, Guanzheng Chen, Xin	906
851	method for better instruction tuning. <i>arXiv preprint</i>	Li, Shijian Lu, Chunyan Miao, and Lidong Bing.	907
852	<i>arXiv:2309.02301</i> .	2024. Mitigating object hallucinations in large vision-	908
853	Qidong Huang, Xiaoyi Dong, Pan Zhang, Bin Wang,	language models through visual contrastive decod-	909
854	Conghui He, Jiaqi Wang, Dahua Lin, Weiming	ing. In <i>Proceedings of the IEEE/CVF Conference</i>	910
855	Zhang, and Nenghai Yu. 2024a. Opera: Alleviating	<i>on Computer Vision and Pattern Recognition</i> , pages	911
856	hallucination in multi-modal large language models	13872–13882.	912
857	via over-trust penalty and retrospection-allocation.	Lei Li, Zhihui Xie, Mukai Li, Shunian Chen, Peiyi	913
858	In <i>Proceedings of the IEEE/CVF Conference on Com-</i>	Wang, Liang Chen, Yazheng Yang, Benyou Wang,	914
859	<i>puter Vision and Pattern Recognition</i> , pages 13418–	and Lingpeng Kong. 2023a. Silkie: Preference dis-	915
860	13427.	tillation for large visual language models. <i>arXiv</i>	916
		<i>preprint arXiv:2312.10665</i> .	917

918	Wei Li, Zhen Huang, Houqiang Li, Le Lu, Yang Lu,	In <i>ICASSP 2020-2020 IEEE International Confer-</i>	972
919	Xinmei Tian, Xu Shen, and Jieping Ye. 2024a. Vi-	<i>ence on Acoustics, Speech and Signal Processing</i>	973
920	visual evidence prompting mitigates hallucinations in	( <i>ICASSP</i> ), pages 8129–8133. IEEE.	974
921	multimodal large language models.		
922	Yifan Li, Yifan Du, Kun Zhou, Jinpeng Wang,	Adyasha Maharana, Amita Kamath, Christopher Clark,	975
923	Wayne Xin Zhao, and Ji-Rong Wen. 2023b. Eval-	Mohit Bansal, and Aniruddha Kembhavi. 2023. Ex-	976
924	uating object hallucination in large vision-language	posing and addressing cross-task inconsistency in	977
925	models. <i>arXiv preprint arXiv:2305.10355</i> .	unified vision-language models. <i>arXiv preprint</i>	978
		<i>arXiv:2303.16133</i> .	979
926	Zhang Li, Biao Yang, Qiang Liu, Zhiyin Ma, Shuo	Mayug Maniparambil, Raiymbek Akshulakov, Yasser	980
927	Zhang, Jingxu Yang, Yabo Sun, Yuliang Liu, and	Abdelaziz Dahou Djilali, Mohamed El Amine Seddik,	981
928	Xiang Bai. 2024b. Monkey: Image resolution and	Sanath Narayan, Kartikeya Mangalam, and Noel E	982
929	text label are important things for large multi-modal	O’Connor. 2024. Do vision and language encoders	983
930	models. In <i>Proceedings of the IEEE/CVF Conference</i>	represent the world similarly? In <i>Proceedings of</i>	984
931	<i>on Computer Vision and Pattern Recognition</i> , pages	<i>the IEEE/CVF Conference on Computer Vision and</i>	985
932	26763–26773.	<i>Pattern Recognition</i> , pages 14334–14343.	986
933	Zhiyuan Li, Dongnan Liu, Chaoyi Zhang, Heng Wang,	Meta AI. 2024. <a href="#">Llama 3.2: Revolutionizing edge AI</a>	987
934	Tengfei Xue, and Weidong Cai. 2024c. Enhancing	<a href="#">and vision with open, customizable models</a> . <i>Meta AI</i>	988
935	advanced visual reasoning ability of large language	<i>Blog</i> . Retrieved December 20, 2024.	989
936	models. <i>arXiv preprint arXiv:2409.13980</i> .		
937	Victor Weixin Liang, Yuhui Zhang, Yongchan Kwon,	Kyungmin Min, Minbeom Kim, Kang-il Lee, Don-	990
938	Serena Yeung, and James Y Zou. 2022. Mind the gap:	gryeol Lee, and Kyomin Jung. 2024. Mitigat-	991
939	Understanding the modality gap in multi-modal con-	ing hallucinations in large vision-language mod-	992
940	trastive representation learning. <i>Advances in Neural</i>	els via summary-guided decoding. <i>arXiv preprint</i>	993
941	<i>Information Processing Systems</i> , 35:17612–17625.	<i>arXiv:2410.13321</i> .	994
942	Fuxiao Liu, Kevin Lin, Linjie Li, Jianfeng Wang, Yaser	Clement Neo, Luke Ong, Philip Torr, Mor Geva, David	995
943	Yacoob, and Lijuan Wang. 2023. Mitigating halluci-	Krueger, and Fazl Barez. 2024. Towards interpret-	996
944	ation in large multi-modal models via robust instruc-	ing visual information processing in vision-language	997
945	tion tuning. In <i>The Twelfth International Conference</i>	models. <i>arXiv preprint arXiv:2410.07149</i> .	998
946	<i>on Learning Representations</i> .		
947	Hanchao Liu, Wenyuan Xue, Yifei Chen, Dapeng Chen,	OpenAI. Chatgpt can now see, hear, and	999
948	Xiutian Zhao, Ke Wang, Liping Hou, Rongjun Li,	speak. <a href="https://openai.com/index/chatgpt-can-now-see-hear-and-speak/">https://openai.com/index/</a>	1000
949	and Wei Peng. 2024a. A survey on hallucination	<a href="https://openai.com/index/chatgpt-can-now-see-hear-and-speak/">chatgpt-can-now-see-hear-and-speak/</a> .	1001
950	in large vision-language models. <i>arXiv preprint</i>	Accessed: September 25, 2023.	1002
951	<i>arXiv:2402.00253</i> .		
952	Haotian Liu, Chunyuan Li, Qingyang Wu, and Yong Jae	Yassine Ouali, Adrian Bulat, Brais Martinez, and	1003
953	Lee. 2024b. Visual instruction tuning. <i>Advances in</i>	Georgios Tzimiropoulos. 2025. Clip-dpo: Vision-	1004
954	<i>neural information processing systems</i> , 36.	language models as a source of preference for fixing	1005
955	Sheng Liu, Haotian Ye, and James Zou. 2024c.	hallucinations in lvlms. In <i>European Conference on</i>	1006
956	Reducing hallucinations in vision-language mod-	<i>Computer Vision</i> , pages 395–413. Springer.	1007
957	els via latent space steering. <i>arXiv preprint</i>		
958	<i>arXiv:2410.15778</i> .	Dongmin Park, Zhaofang Qian, Guangxing Han, and	1008
959	Shi Liu, Kecheng Zheng, and Wei Chen. Paying more	Ser-Nam Lim. 2024. Mitigating dialogue halluci-	1009
960	attention to image: A training-free method for allevi-	ation for large multi-modal models via adversarial	1010
961	ating hallucination in lvlms, 2024. URL <a href="https://arxiv.org/abs/2407.21771">https://arxiv.</a>	instruction tuning. <i>arXiv preprint arXiv:2403.10492</i> .	1011
962	<i>org/abs/2407.21771</i> .		
963	Yangzhou Liu, Yue Cao, Zhangwei Gao, Weiyun Wang,	Xiaoye Qu, Qiyuan Chen, Wei Wei, Jishuo Sun, and	1012
964	Zhe Chen, Wenhai Wang, Hao Tian, Lewei Lu,	Jianfeng Dong. 2024. Alleviating hallucination in	1013
965	Xizhou Zhu, Tong Lu, et al. 2024d. Mminstruct: A	large vision-language models with active retrieval	1014
966	high-quality multi-modal instruction tuning dataset	augmentation. <i>arXiv preprint arXiv:2408.00555</i> .	1015
967	with extensive diversity. <i>Science China Information</i>		
968	<i>Sciences</i> , 67(12):1–16.	Alec Radford, Jong Wook Kim, Chris Hallacy, Aditya	1016
969	Rao Ma, Lesheng Jin, Qi Liu, Lu Chen, and Kai Yu.	Ramesh, Gabriel Goh, Sandhini Agarwal, Girish Sas-	1017
970	2020. Addressing the polysemy problem in language	try, Amanda Askell, Pamela Mishkin, Jack Clark,	1018
971	modeling with attentional multi-sense embeddings.	et al. 2021. Learning transferable visual models from	1019
		natural language supervision. In <i>International confer-</i>	1020
		<i>ence on machine learning</i> , pages 8748–8763. PMLR.	1021
		Rita Ramos, Bruno Martins, and Desmond Elliott.	1022
		2023a. Lmcap: Few-shot multilingual image caption-	1023
		ing by retrieval augmented language model prompt-	1024
		ing. <i>arXiv preprint arXiv:2305.19821</i> .	1025



1026	Rita Ramos, Bruno Martins, Desmond Elliott, and Yova Kementchedjheva. 2023b. Smallcap: lightweight image captioning prompted with retrieval augmentation. In <i>Proceedings of the IEEE/CVF Conference on Computer Vision and Pattern Recognition</i> , pages 2840–2849.	Azhar, et al. 2023a. Llama: Open and efficient foundation language models. <i>arXiv preprint arXiv:2302.13971</i> .	1081
1027			1082
1028			1083
1029			
1030		Hugo Touvron, Louis Martin, Kevin Stone, Peter Albert, Amjad Almahairi, Yasmine Babaei, Nikolay Bashlykov, Soumya Batra, Prajjwal Bhargava, Shruti Bhosale, et al. 2023b. Llama 2: Open foundation and fine-tuned chat models. <i>arXiv preprint arXiv:2307.09288</i> .	1084
1031			1085
1032	Anna Rohrbach, Lisa Anne Hendricks, Kaylee Burns, Trevor Darrell, and Kate Saenko. 2018. Object hallucination in image captioning. <i>arXiv preprint arXiv:1809.02156</i> .		1086
1033			1087
1034			1088
1035			1089
1036	Sara Sarto, Marcella Cornia, Lorenzo Baraldi, Alessandro Nicolosi, and Rita Cucchiara. 2024. Towards retrieval-augmented architectures for image captioning. <i>ACM Transactions on Multimedia Computing, Communications and Applications</i> .	Chenglong Wang, Yang Gan, Yifu Huo, Yongyu Mu, Murun Yang, Qiaozhi He, Tong Xiao, Chunliang Zhang, Tongran Liu, Quan Du, et al. 2024a. Rovrm: A robust visual reward model optimized via auxiliary textual preference data. <i>arXiv preprint arXiv:2408.12109</i> .	1090
1037			1091
1038			1092
1039			1093
1040			1094
1041	Yuying Shang, Xinyi Zeng, Yutao Zhu, Xiao Yang, Zhengwei Fang, Jingyuan Zhang, Jiawei Chen, Zinan Liu, and Yu Tian. 2024. From pixels to tokens: Revisiting object hallucinations in large vision-language models. <i>arXiv preprint arXiv:2410.06795</i> .		1095
1042		Chenxi Wang, Xiang Chen, Ningyu Zhang, Bozhong Tian, Haoming Xu, Shumin Deng, and Huajun Chen. 2024b. Mllm can see? dynamic correction decoding for hallucination mitigation. <i>arXiv preprint arXiv:2410.11779</i> .	1096
1043			1097
1044			1098
1045			1099
1046	Pratyusha Sharma, Tamar Rott Shaham, Manel Baradad, Stephanie Fu, Adrian Rodriguez-Munoz, Shivam Duggal, Phillip Isola, and Antonio Torralba. 2024. A vision check-up for language models. In <i>Proceedings of the IEEE/CVF Conference on Computer Vision and Pattern Recognition</i> , pages 14410–14419.		1100
1047		Junyang Wang, Yiyang Zhou, Guohai Xu, Pengcheng Shi, Chenlin Zhao, Haiyang Xu, Qinghao Ye, Ming Yan, Ji Zhang, Jihua Zhu, et al. 2023. Evaluation and analysis of hallucination in large vision-language models. <i>arXiv preprint arXiv:2308.15126</i> .	1101
1048			1102
1049			1103
1050			1104
1051			1105
1052	Zhelun Shi, Zhipin Wang, Hongxing Fan, Zaibin Zhang, Lijun Li, Yongting Zhang, Zhenfei Yin, Lu Sheng, Yu Qiao, and Jing Shao. 2024. Assessment of multimodal large language models in alignment with human values. <i>arXiv preprint arXiv:2403.17830</i> .	Lei Wang, Jiabang He, Shenshen Li, Ning Liu, and Ee-Peng Lim. 2024c. Mitigating fine-grained hallucination by fine-tuning large vision-language models with caption rewrites. In <i>International Conference on Multimedia Modeling</i> , pages 32–45. Springer.	1106
1053			1107
1054			1108
1055			1109
1056			1110
1057	Dong Shu, Bingbing Duan, Kai Guo, Kaixiong Zhou, Jiliang Tang, and Mengnan Du. 2024. Exploring the alignment landscape: Llms and geometric deep models in protein representation. <i>arXiv preprint arXiv:2411.05316</i> .	Peng Wang, Shuai Bai, Sinan Tan, Shijie Wang, Zhihao Fan, Jinze Bai, Keqin Chen, Xuejing Liu, Jialin Wang, Wenbin Ge, et al. 2024d. Qwen2-vl: Enhancing vision-language model’s perception of the world at any resolution. <i>arXiv preprint arXiv:2409.12191</i> .	1111
1058			1112
1059			1113
1060			1114
1061			1115
1062	Zhiqing Sun, Sheng Shen, Shengcao Cao, Haotian Liu, Chunyuan Li, Yikang Shen, Chuang Gan, Liang-Yan Gui, Yu-Xiong Wang, Yiming Yang, et al. 2023. Aligning large multimodal models with factually augmented rlhf. <i>arXiv preprint arXiv:2309.14525</i> .	Xintong Wang, Jingheng Pan, Liang Ding, and Chris Biemann. 2024e. Mitigating hallucinations in large vision-language models with instruction contrastive decoding. <i>arXiv preprint arXiv:2403.18715</i> .	1116
1063			1117
1064			1118
1065			1119
1066			
1067	Jingqun Tang, Chunhui Lin, Zhen Zhao, Shu Wei, Binghong Wu, Qi Liu, Hao Feng, Yang Li, Siqi Wang, Lei Liao, et al. 2024. Textsquare: Scaling up text-centric visual instruction tuning. <i>arXiv preprint arXiv:2404.12803</i> .	Sangmin Woo, Jaehyuk Jang, Donguk Kim, Yubin Choi, and Changick Kim. 2024a. Ritual: Random image transformations as a universal anti-hallucination lever in lvlms. <i>arXiv preprint arXiv:2405.17821</i> .	1120
1068			1121
1069			1122
1070			1123
1071			
1072	Gemini Team, Rohan Anil, Sebastian Borgeaud, Jean-Baptiste Alayrac, Jiahui Yu, Radu Soricut, Johan Schalkwyk, Andrew M Dai, Anja Hauth, Katie Millican, et al. 2023. Gemini: a family of highly capable multimodal models. <i>arXiv preprint arXiv:2312.11805</i> .	Sangmin Woo, Donguk Kim, Jaehyuk Jang, Yubin Choi, and Changick Kim. 2024b. Don’t miss the forest for the trees: Attentional vision calibration for large vision language models. <i>arXiv preprint arXiv:2405.17820</i> .	1124
1073			1125
1074			1126
1075			1127
1076			1128
1077			
1078	Hugo Touvron, Thibaut Lavril, Gautier Izacard, Xavier Martinet, Marie-Anne Lachaux, Timothée Lacroix, Baptiste Rozière, Naman Goyal, Eric Hambro, Faisal	Junfei Wu, Qiang Liu, Ding Wang, Jinghao Zhang, Shu Wu, Liang Wang, and Tieniu Tan. 2024a. Logical closed loop: Uncovering object hallucinations in large vision-language models. <i>arXiv preprint arXiv:2402.11622</i> .	1129
1079			1130
1080			1131
			1132
			1133

1134	Mingrui Wu, Jiayi Ji, Oucheng Huang, Jiale Li, Yuhang	Chung-En (Johnny) Yu, Brian Jalaian, and Nathaniel D.	1190
1135	Wu, Xiaoshuai Sun, and Rongrong Ji. 2024b. Eval-	Bastian. 2024a. <a href="#">Mitigating large vision-language</a>	1191
1136	uating and analyzing relationship hallucinations	<a href="#">model hallucination at post-hoc via multi-agent sys-</a>	1192
1137	in large vision-language models. <i>arXiv preprint</i>	<a href="#">tem</a> . <i>Proceedings of the AAAI Symposium Series</i> ,	1193
1138	<i>arXiv:2406.16449</i> .	4(1):110–113.	1194
1139	Zhiyu Wu, Xiaokang Chen, Zizheng Pan, Xingchao	Qifan Yu, Juncheng Li, Longhui Wei, Liang Pang, Wen-	1195
1140	Liu, Wen Liu, Damai Dai, Huazuo Gao, Yiyang Ma,	tao Ye, Bosheng Qin, Siliang Tang, Qi Tian, and	1196
1141	Chengyue Wu, Bingxuan Wang, Zhenda Xie, Yu Wu,	Yueting Zhuang. 2024b. Hallucidoctor: Mitigating	1197
1142	Kai Hu, Jiawei Wang, Yaofeng Sun, Yukun Li, Yishi	hallucinatory toxicity in visual instruction data. In	1198
1143	Piao, Kang Guan, Aixin Liu, Xin Xie, Yuxiang You,	<i>Proceedings of the IEEE/CVF Conference on Com-</i>	1199
1144	Kai Dong, Xingkai Yu, Haowei Zhang, Liang Zhao,	<i>puter Vision and Pattern Recognition</i> , pages 12944–	1200
1145	Yisong Wang, and Chong Ruan. 2024c. <a href="#">Deepseek-</a>	12953.	1201
1146	<a href="#">v12: Mixture-of-experts vision-language models</a>		
1147	<a href="#">for advanced multimodal understanding</a> . <i>Preprint</i> ,	Tianyu Yu, Yuan Yao, Haoye Zhang, Taiwen He, Yifeng	1202
1148	<i>arXiv:2412.10302</i> .	Han, Ganqu Cui, Jinyi Hu, Zhiyuan Liu, Hai-Tao	1203
1149	Wenyi Xiao, Ziwei Huang, Leilei Gan, Wanggui He,	Zheng, Maosong Sun, et al. 2024c. RLhf-v: Towards	1204
1150	Haoyuan Li, Zhelun Yu, Hao Jiang, Fei Wu, and Lin-	trustworthy mllms via behavior alignment from fine-	1205
1151	chao Zhu. 2024. Detecting and mitigating hallucina-	grained correctional human feedback. In <i>Proceed-</i>	1206
1152	tion in large vision language models via fine-grained	<i>ings of the IEEE/CVF Conference on Computer Vi-</i>	1207
1153	ai feedback. <i>arXiv preprint arXiv:2404.14233</i> .	<i>sion and Pattern Recognition</i> , pages 13807–13816.	1208
1154	Yuxi Xie, Guanzhen Li, Xiao Xu, and Min-Yen Kan.	Zihao Yue, Liang Zhang, and Qin Jin. 2024. Less	1209
1155	2024. V-dpo: Mitigating hallucination in large vision	is more: Mitigating multimodal hallucination from	1210
1156	language models via vision-guided direct preference	an eos decision perspective. <i>arXiv preprint</i>	1211
1157	optimization. <i>arXiv preprint arXiv:2411.02712</i> .	<i>arXiv:2402.14545</i> .	1212
1158	Peng Xu, Wenqi Shao, Kaipeng Zhang, Peng Gao,	Bohan Zhai, Shijia Yang, Xiangchen Zhao, Chenfeng	1213
1159	Shuo Liu, Meng Lei, Fanqing Meng, Siyuan Huang,	Xu, Sheng Shen, Dongdi Zhao, Kurt Keutzer, Man-	1214
1160	Yu Qiao, and Ping Luo. 2024. Lvlm-ehub: A com-	ling Li, Tan Yan, and Xiangjun Fan. 2023. Halle-	1215
1161	prehensive evaluation benchmark for large vision-	switch: Rethinking and controlling object existence	1216
1162	language models. <i>IEEE Transactions on Pattern</i>	hallucinations in large vision language models for	1217
1163	<i>Analysis and Machine Intelligence</i> .	detailed caption. <i>arXiv preprint arXiv:2310.01779</i> .	1218
1164	An Yan, Zhengyuan Yang, Junda Wu, Wanrong Zhu,	Jinrui Zhang, Teng Wang, Haigang Zhang, Ping Lu,	1219
1165	Jianwei Yang, Linjie Li, Kevin Lin, Jianfeng Wang,	and Feng Zheng. 2025. Reflective instruction tuning:	1220
1166	Julian McAuley, Jianfeng Gao, et al. 2024. List	Mitigating hallucinations in large vision-language	1221
1167	items one by one: A new data source and learn-	models. In <i>European Conference on Computer Vi-</i>	1222
1168	ing paradigm for multimodal llms. <i>arXiv preprint</i>	<i>sion</i> , pages 196–213. Springer.	1223
1169	<i>arXiv:2404.16375</i> .	Yanan Zhang, Jiangmeng Li, Lixiang Liu, and Wenwen	1224
1170	Dingchen Yang, Bowen Cao, Guang Chen, and	Qiang. 2024. Rethinking misalignment in vision-	1225
1171	Changjun Jiang. 2024. Pensieve: Retrospect-then-	language model adaptation from a causal perspective.	1226
1172	compare mitigates visual hallucination. <i>arXiv</i>	<i>arXiv preprint arXiv:2410.12816</i> .	1227
1173	<i>preprint arXiv:2403.14401</i> .	Haiyan Zhao, Hanjie Chen, Fan Yang, Ninghao Liu,	1228
1174	Jinyu Yang, Jiali Duan, Son Tran, Yi Xu, Sampath	Huiqi Deng, Hengyi Cai, Shuaiqiang Wang, Dawei	1229
1175	Chanda, Liqun Chen, Belinda Zeng, Trishul Chilimbi,	Yin, and Mengnan Du. 2024a. Explainability for	1230
1176	and Junzhou Huang. 2022. Vision-language pre-	large language models: A survey. <i>ACM Transactions</i>	1231
1177	training with triple contrastive learning. In <i>Proceed-</i>	<i>on Intelligent Systems and Technology</i> , 15(2):1–38.	1232
1178	<i>ings of the IEEE/CVF Conference on Computer Vi-</i>	Haiyan Zhao, Fan Yang, Himabindu Lakkaraju, and	1233
1179	<i>sion and Pattern Recognition</i> , pages 15671–15680.	Mengnan Du. 2024b. Towards uncovering how large	1234
1180	Shukang Yin, Chaoyou Fu, Sirui Zhao, Tong Xu, Hao	language model works: An explainability perspective.	1235
1181	Wang, Dianbo Sui, Yunhang Shen, Ke Li, Xing Sun,	<i>arXiv e-prints</i> , pages arXiv–2402.	1236
1182	and Enhong Chen. 2023. Woodpecker: Hallucina-	Haiyan Zhao, Heng Zhao, Bo Shen, Ali Payani, Fan	1237
1183	tion correction for multimodal large language models.	Yang, and Mengnan Du. 2024c. Beyond single	1238
1184	<i>arXiv preprint arXiv:2310.16045</i> .	concept vector: Modeling concept subspace in	1239
1185	Haoxuan You, Haotian Zhang, Zhe Gan, Xianzhi Du,	llms with gaussian distribution. <i>arXiv preprint</i>	1240
1186	Bowen Zhang, Zirui Wang, Liangliang Cao, Shih-Fu	<i>arXiv:2410.00153</i> .	1241
1187	Chang, and Yinfei Yang. 2023. Ferret: Refer and	Linxi Zhao, Yihe Deng, Weitong Zhang, and Quanquan	1242
1188	ground anything anywhere at any granularity. <i>arXiv</i>	Gu. 2024d. Mitigating object hallucination in large	1243
1189	<i>preprint arXiv:2310.07704</i> .	vision-language models via classifier-free guidance.	1244
		<i>arXiv preprint arXiv:2402.08680</i> .	1245

Tianyi Zhao, Liangliang Zhang, Yao Ma, and Lu Cheng. 2024e. A survey on safe multi-modal learning systems. In *Proceedings of the 30th ACM SIGKDD Conference on Knowledge Discovery and Data Mining*, pages 6655–6665.

Yongqiang Zhao, Zhenyu Li, Zhi Jin, Feng Zhang, Haiyan Zhao, Chengfeng Dou, Zhengwei Tao, Xinhai Xu, and Donghong Liu. 2023a. Enhancing the spatial awareness capability of multi-modal large language model. *arXiv preprint arXiv:2310.20357*.

Zhiyuan Zhao, Bin Wang, Linke Ouyang, Xiaoyi Dong, Jiaqi Wang, and Conghui He. 2023b. Beyond hallucinations: Enhancing lvlms through hallucination-aware direct preference optimization. *arXiv preprint arXiv:2311.16839*.

Weihong Zhong, Xiaocheng Feng, Liang Zhao, Qiming Li, Lei Huang, Yuxuan Gu, Weitao Ma, Yuan Xu, and Bing Qin. 2024. Investigating and mitigating the multimodal hallucination snowballing in large vision-language models. *arXiv preprint arXiv:2407.00569*.

Da-Wei Zhou, Yuanhan Zhang, Jingyi Ning, Han-Jia Ye, De-Chuan Zhan, and Ziwei Liu. 2023a. Learning without forgetting for vision-language models. *arXiv preprint arXiv:2305.19270*.

Yiyang Zhou, Chenhang Cui, Rafael Rafailov, Chelsea Finn, and Huaxiu Yao. 2024. Aligning modalities in vision large language models via preference fine-tuning. *arXiv preprint arXiv:2402.11411*.

Yiyang Zhou, Chenhang Cui, Jaehong Yoon, Linjun Zhang, Zhun Deng, Chelsea Finn, Mohit Bansal, and Huaxiu Yao. 2023b. Analyzing and mitigating object hallucination in large vision-language models. *arXiv preprint arXiv:2310.00754*.

Deyao Zhu, Jun Chen, Xiaoqian Shen, Xiang Li, and Mohamed Elhoseiny. 2023. Minigpt-4: Enhancing vision-language understanding with advanced large language models. *arXiv preprint arXiv:2304.10592*.

Lanyun Zhu, Deyi Ji, Tianrun Chen, Peng Xu, Jieping Ye, and Jun Liu. 2024a. Ibd: Alleviating hallucinations in large vision-language models via image-biased decoding. *arXiv preprint arXiv:2402.18476*.

Tinghui Zhu, Qin Liu, Fei Wang, Zhengzhong Tu, and Muhao Chen. 2024b. Unraveling cross-modality knowledge conflicts in large vision-language models. *arXiv preprint arXiv:2410.03659*.



## A Overview of LVLM Architectures

Table 1 summarizes the architectural components of six prominent LVLMs discussed throughout this survey paper on model alignment and misalignment. The comparison reveals common patterns in LVLM design: transformer-based vision encoders (predominantly ViT variants), adapter modules of varying complexity to connect vision and language components, and state-of-the-art language models.

## B How to Measure Alignment?

This section examines approaches for quantifying the effectiveness of alignment in LVLMs. These measurement approaches naturally align with our earlier definition in Section 2.1 of representation alignment and behavioral alignment, and can be organized along these two fundamental levels.

**Representation Level.** At the representation level, alignment can be directly measured between visual and textual representations within the LVLM’s embedding space by assessing how similarly the visual and textual modalities encode and relate to the same concepts or data points. The simplest approach is to compute the cosine similarity between the embeddings of visual and textual data. High alignment corresponds to scores close to 1, while low alignment corresponds to scores closer to 0 (Shu et al., 2024). More sophisticated metrics have been developed to assess alignment between the two representation spaces. For instance, the mutual nearest-neighbor metric quantifies alignment by evaluating the consistency of nearest neighbors across modalities (Huh et al., 2024). Another approach is kernel alignment, which evaluates the similarity of pairwise relationships within each modality’s embedding space, providing a holistic view of the alignment structure (Maniparambil et al., 2024).

**Behavioral Level.** The behavioral level measures alignment through the model’s performance on various downstream tasks and benchmarks, using both direct comparisons and automated evaluation systems. The strength of alignment directly impacts the LVLM’s performance, as better alignment typically leads to improved task outcomes. These measurements generally involve comparing the model’s outputs against ground truth labels, either through direct comparison or using evaluation models to simulate human judgment. Numerous benchmarks have been developed to assess LVLM alignment

across a range of tasks, from coarse-grained evaluations (e.g., object existence) to fine-grained assessments (e.g., color, count, spatial relations). Examples of such benchmarks include POPE (Li et al., 2023b), CHAIR (Rohrbach et al., 2018), MME (Fu et al., 2023), MMHal-Bench (Sun et al., 2023), and LLaVa-Bench (Liu et al., 2024b). In addition to traditional benchmarks, advanced evaluation models like GAVIE (Liu et al., 2023), CCEval (Zhai et al., 2023) and HaELM (Wang et al., 2023) provide sophisticated assessments by considering context and evaluating responses comprehensively, similar to human evaluators. The flexibility and diversity of evaluation models enable thorough measurement capabilities needed for open-ended questions.

In Table 2, we compare several existing benchmarks. While most of these benchmarks focus on evaluating misalignment, some also assess reasoning capabilities, such as whether the LVLM can reason based on image information or whether the LVLM fully follow user input instructions. Future benchmarks should also adopt this comprehensive approach, evaluating not only misalignment but also whether mitigating misalignment impacts the LVLM’s reasoning ability, as our goal is to develop LVLMs with minimal misalignment while preserving their reasoning capabilities.

## C More Reasons for Misalignment

Beyond the dataset-level issues discussed in Section 3.2.1, we present additional dataset-related challenges that may contribute to the misalignment of LVLMs.

- **Data Imbalance:** When certain classes or types of data are disproportionately represented, it skews the model’s training process (Liu et al., 2023; Hu et al., 2023). For example, visual question-answering datasets often overrepresent positive answers, subtly training the model to favor these outcomes while underperforming on underrepresented negative answers.
- **Data Inconsistency:** Inconsistencies exacerbate misalignment by introducing contradictory outputs across different tasks for the same image. For instance, an image captioning task might describe an image as depicting ‘a tiger eating a chicken,’ yet in a visual question-answering task for the same image, the answer to ‘what is the tiger eating?’ might label the prey as ‘a duck’ (Maharana et al., 2023). Such contradictions disrupt the model’s ability to generate coherent and

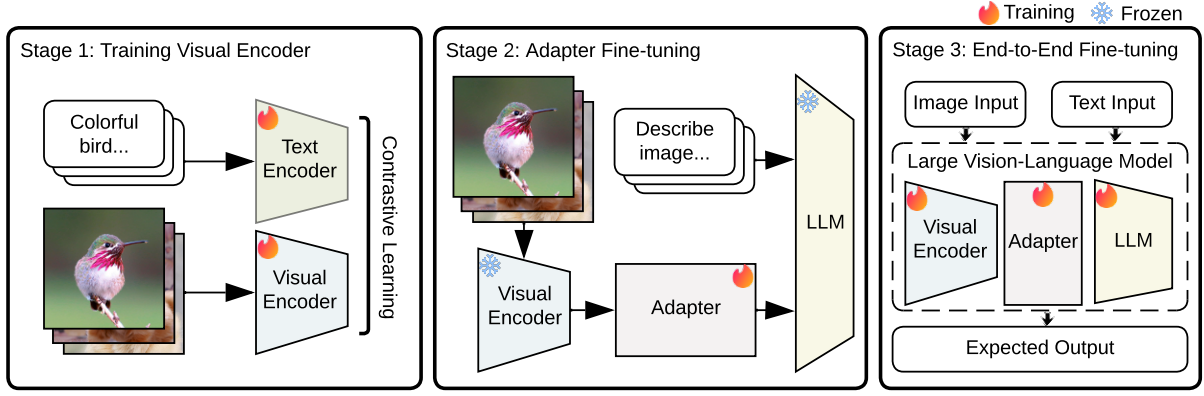


Figure 3: Overview of the three-stage LVLM training process, showing the progression from contrastive learning of visual-text encoders, through adapter fine-tuning with frozen components, to end-to-end model training.

Table 1: Comparison of Vision-Language Models

	Vision Encoder	Adapter	LLM
<b>Qwen-VL</b> (Bai et al., 2023b)	Vision Transformer (ViT)	Single cross-attention layer	Qwen
<b>Qwen2-VL</b> (Wang et al., 2024d)	ViT	MLP layer	Qwen2
<b>MiniGPT-4</b> (Zhu et al., 2023)	ViT-G/14	Single linear projection layer	Vicuna
<b>Llama 3.2-Vision</b> (Meta AI, 2024)	Modified ViT (16×16 patches)	Multiple cross-attention layers	Llama 3.1 text-only model
<b>LLaVA-1.5</b> (Liu et al., 2024b)	CLIP-ViT-L-336px	MLP projection layer	Vicuna v1.5
<b>DeepSeek-VL2</b> (Wu et al., 2024c)	SigLIP-SO400M-384	Two-layer MLP	DeepSeekMoE

consistent outputs across tasks.

- **Data False Negative:** False negatives in the dataset further complicate alignment, as negative image-text pairs, though not perfectly matching, share overlapping components (Liang et al., 2022; Byun et al., 2024). During training, embeddings of positive pairs are drawn closer together, while those of negative pairs are pushed apart. This binary method can suppress latent similarities within false negatives, reducing the model’s capacity to effectively align diverse modalities.
- **Data Polysemy:** The inherent polysemy within datasets introduces additional complexity. Polysemy enriches data diversity by allowing a single word or image to convey multiple meanings depending on context, but this ambiguity also amplifies the risk of misalignment (Ma et al., 2020; Ding and Van Noord). For example, an image caption of ‘the bat hit the ball’ could refer to the animal or the baseball bat. This variability challenges the model to establish consistent mappings between modalities.

## D Examples of LVLM Descriptions

In this section, we present examples from four leading LVLMs and illustrate their generated descriptions for given images. We have selected

one closed-source model, ChatGPT-4o, accessed through its official website <https://chatgpt.com/>, and three open-source models, Qwen2-VL-72B-Instruct, DeepSeek-VL2, and LLaVa-1.5-13B-hf, loaded directly from Hugging Face. All implementation settings, including parameters such as temperature, were kept at their default values to ensure consistency. The experiments were conducted using an A100 PCIE 80GB GPU. To enhance computational efficiency and performance, the models were loaded in float16 precision. During the evaluation phase, each model was provided with an image along with the following prompt: ‘Describe this image in detail. Include specific objects, their attributes, and relationships.’ The input images and the corresponding descriptions generated by each model are presented in Figure 4, 5, and 6.

## E Mitigation Methods Comparison

As shown in Table 3, we selected LLaVa-V1.5-7B as the baseline model and evaluated it on POPE benchmarks. We then tested three mitigation methods: SoM-LLaVA (Yan et al., 2024), SID (Huo et al., 2024), and LogicCheckGPT (Wu et al., 2024a), to assess their effectiveness and efficiency in mitigating misalignment in the baseline model. The baseline model was loaded directly from Hugging Face, with parameters in float16 precision

Table 2: Comparison of Misalignment Benchmark across Different Evaluation Dimensions. The evaluation dimensions are categorized into two main aspects: (1) Evaluating misalignment, which examines object, attribute, and relational misalignments in model outputs; and (2) Evaluating reasoning, which assesses models’ cognitive reasoning abilities and instruction following capabilities. The rightmost column indicates whether the benchmark uses traditional evaluation methods or third-model evaluation approaches.

	Evaluating Misalignment			Evaluating Reasoning		Traditional/ Third-model
	Object Misalignment	Attribute Misalignment	Relational Misalignment	Cognition Reasoning	Instruction Following	
POPE (Li et al., 2023b)	✓	✗	✗	✗	✗	Traditional
CHAIR (Rohrbach et al., 2018)	✓	✗	✗	✗	✗	Traditional
MME (Fu et al., 2023)	✓	✓	✓	✓	✗	Traditional
MMHal-Bench (Sun et al., 2023)	✓	✓	✓	✓	✗	Traditional
LLaVa-Bench (Liu et al., 2024b)	✓	✓	✓	✗	✗	Traditional
LVLm-eHub (Xu et al., 2024)	✓	✓	✗	✓	✗	Traditional
GAVIE (Liu et al., 2023)	✓	✓	✓	✗	✓	Third-model
CCEval (Zhai et al., 2023)	✓	✗	✗	✗	✗	Third-model
HaELM (Wang et al., 2023)	✓	✓	✓	✗	✗	Third-model

Table 3: Comparison of Mitigation Methods on the POPE Benchmark. The table demonstrates the performance of the baseline model and different mitigation methods that address baseline misalignment. Performance is evaluated using Accuracy, Precision, Recall, and F1 score (with the highest score in each category underlined). Additionally, the computational cost (in seconds per input) for both the baseline and each mitigation method is provided.

Method	POPE-Random				POPE-Adversarial				POPE-Popular				Comp. Cost
	Acc	Precis	Recall	F1	Acc	Precis	Recall	F1	Acc	Precis	Recall	F1	Sec/Input
<b>Baseline</b> LLaVa-V1.5-7B	88.4	87.5	89.7	88.6	77.9	72.6	89.7	80.3	84.8	81.7	89.7	85.5	1.27
<b>Mitigations</b>													
SoM-LLaVA (Yan et al., 2024)	<u>89.6</u>	89.1	<u>90.2</u>	<u>89.6</u>	81.0	76.2	<u>90.2</u>	82.6	84.8	81.4	<u>90.2</u>	85.6	1.62
SID (Huo et al., 2024)	89.4	92.2	86.1	89.0	80.4	77.4	85.9	81.4	85.9	85.9	85.9	<u>85.9</u>	1.68
LogicCheckGPT (Wu et al., 2024a)	88.0	<u>98.3</u>	77.3	86.5	<u>85.0</u>	<u>94.1</u>	74.7	<u>83.3</u>	<u>86.7</u>	<u>95.1</u>	77.3	85.3	51.5

and all other implementation details set to default. Each mitigation method was implemented strictly according to its official GitHub repository, without modifications to core components, except for necessary adjustments such as path configurations.

We evaluated model performance using Accuracy, Precision, Recall, and F1-score, with the highest values underlined in the table. The results indicate that mitigation methods generally improve performance across most metrics compared to the baseline, particularly SoM-LLaVA and LogicCheckGPT, which achieved five and six highest scores, respectively. However, a deeper analysis reveals that some methods negatively impacted certain metrics. For instance, while LogicCheckGPT achieved the highest Precision on all benchmarks, it exhibited relatively lower Recall and F1 scores, sometimes even worse than the baseline. This occurs because LogicCheckGPT is conservative in predicting positives, meaning it only classifies a sample as positive when it is highly confident, resulting in fewer false positives but more false negatives. Interestingly, SoM-LLaVA consistently achieved the highest Recall across all benchmarks, indicating that it is less strict in determining positive cases

compared to LogicCheckGPT. This highlights how different mitigation strategies lead to different prediction behaviors, emphasizing the need for future works to report performance across multiple metrics rather than focusing solely on a single high-performing metric.

Beyond performance, we also evaluated the computational cost of each mitigation method in seconds per input. While SoM-LLaVA and SID had only a minor increase in inference time compared to the baseline, LogicCheckGPT required significantly more time. This is because LogicCheckGPT relies on an external third model, such as GPT-3.5, to assess logical consistency and mitigate object misalignment, making its computational cost highly dependent on the third model’s complexity. This trade-off between performance and computational efficiency is critical, as high computational time may hinder real-world deployment of mitigation techniques. Future research should aim to balance effectiveness with efficiency to ensure practical usability.



## F Future Research Directions

In this section, we discuss several important directions for future research in understanding and improving alignment in LVLMs.

### F.1 Standardized Benchmarks

The current evaluation of misalignment in LVLMs suffers from a critical limitation, i.e., the lack of standardized, comprehensive benchmarks that can systematically assess different types of misalignment across models. While existing benchmarks have made important contributions, they typically focus on specific aspects of misalignment in isolation. For instance, POPE (Li et al., 2023b) primarily evaluates object hallucination, while other benchmarks concentrate on particular relationship errors or attribute inconsistencies. What is urgently needed is a unified evaluation framework that can systematically assess misalignment across all semantic levels, from object-level (e.g., describing a non-existent dog in an image) to attribute-level (e.g., color, size, texture errors) and relation-level misalignment (e.g., spatial relationship errors). Such a comprehensive benchmark would enable direct comparisons between different LVLM architectures and alignment techniques using standardized metrics, evaluate both representational alignment and behavioral alignment, and assess how misalignment manifests across different types of tasks. The benchmark should also consider both the frequency and severity of different types of misalignment, rather than treating all misalignments as equally problematic. The development of such standardized benchmarks would represent a significant step forward in our understanding of misalignment in LVLMs and accelerate progress toward more reliable and trustworthy vision-language systems.

### F.2 Explainability based Diagnose

To better understand and address alignment issues in LVLMs, future research should leverage advanced explainability techniques that can reveal the internal mechanisms of these models. There are two critical categories of explainability approaches that warrant investigation: (1) internal knowledge decoding and (2) attribution methods.

The first category of explainability approaches centers on internal knowledge decoding and understanding how information is processed within LVLMs (Zhao et al., 2024b,a). Mechanistic interpretability approaches could help identify specific

components and circuits within LVLMs that are responsible for cross-modal alignment, providing insights into how visual and language representations are integrated and processed. Similarly, probing techniques can analyze the emergence and evolution of aligned representations across different layers and attention heads, helping researchers understand where and how misalignment occurs within the model architecture (Zhao et al., 2024c). This detailed understanding of the internal working mechanisms would not only advance theoretical knowledge but also guide the development of more effective alignment techniques.

The second critical category focuses on attribution methods that can determine the relative influence of different information sources on model outputs. LVLMs have three primary information sources for generating outputs: user text prompts, input images, and knowledge stored within pre-trained LLMs. Future research needs to develop sophisticated attribution algorithms that can determine whether a model’s output primarily depends on the input text prompt, derives from the visual information in the image, or relies on the LLM’s internal knowledge. This detailed attribution analysis would help identify when and why misalignment occurs, such as cases where the model inappropriately relies on LLM knowledge rather than visual evidence, or when it fails to properly integrate information from multiple sources. Such insights would be useful for designing targeted mitigation strategies that address specific types of misalignment and improve the overall reliability of LVLMs.

### F.3 Architectural Innovations

Current LVLM architectures face fundamental challenges, including significant ability gaps between visual encoders and LLMs, persistent attention imbalances between modalities, and knowledge conflicts between visual and textual representations. While most existing solutions focus on improving training procedures or adding post-processing steps, future research should focus on architectural innovations that address these structural limitations. This could include developing novel integration mechanisms that better balance the capabilities of visual and language components, and dynamic architectures that can adaptively adjust their attention mechanisms to maintain equilibrium between modalities. The field would benefit from multi-stage processing architectures that explicitly manage knowledge conflicts through specialized

1590 components for different levels of semantic un-  
1591 derstanding. Additionally, new transformer archi-  
1592 tectures specifically designed for vision-language  
1593 tasks, rather than adapted from unimodal architec-  
1594 tures, could help bridge the ability gap between  
1595 visual and textual processing.



#### ChatGPT-4o:

The image showcases a beautifully designed open-concept living room and kitchen area with a modern farmhouse aesthetic... Two dark brown leather armchairs with tufted backrests and wooden armrests face the sofa, each featuring a decorative pillow.... A dark wooden square coffee table sits in the center of the seating arrangement, holding a black bowl with decorative white stones, a potted green plant, a stack of books, and a sculptural decorative object.

The ceiling features exposed dark wooden beams that contrast with the white ceiling, adding a rustic touch to the space. Black recessed ceiling lights are evenly distributed across the ceiling, providing soft illumination... A large island with a wooden top and black barstools sits at the center of the kitchen, complementing the overall color scheme... Decorative elements throughout the space include artwork on the walls, such as a framed black and white photo, a vibrant red abstract piece, and a landscape painting...

#### Qwen2-VL:

This image depicts a modern, open-concept living space with a combination of rustic and contemporary design elements... Lighting: There are several recessed lights installed in the ceiling, providing ample illumination... Sofa: A large, gray sectional sofa is positioned against the wall... Armchairs:... They have tufted backs and are accompanied by small side tables. Coffee Table:... It has a few decorative items on top, including a book, a small bowl, and a vase with greenery... Kitchen Area: A white kitchen island with a marble countertop is visible. It has bar stools tucked under it. Appliances: Stainless steel appliances, including a refrigerator and oven, are integrated into the kitchen design... Front Door: A wooden front door with glass panels is visible...

#### DeepSeek-VL2:

This image depicts a well-designed living room with a modern rustic and cozy interior. The room features a large, dark wooden beams on the ceiling... The room has a large gray sofa with multiple cushions... and a wooden side tables. The room also has a staircase..., and a kitchen area with marble countertops and a large potted plants. The room has a door with glass panels.

#### LLaVa-1.5:

The image depicts a spacious and well-furnished living room with a wooden floor. The room features a couch situated on the left side, a chair on the right side, and a dining table in the center... There are several books scattered around the room, with some on the dining table and others on the floor. A vase can be seen on the dining table, and a remote control is placed nearby. A clock is mounted on the wall, and a bowl is located on the floor. The living room is connected to a kitchen area, which includes a sink and an oven. A staircase can be seen in the background, leading to another floor of the house.

Object Misalignment      Attribute Misalignment      Relational Misalignment

Figure 4: This figure presents examples of descriptions generated by different LVLMs when given the image shown in the upper left corner. The highlighted text segments in the descriptions represent different types of misalignment. Specifically, red highlights indicate object misalignment. Yellow highlights represent attribute misalignment. Blue highlights denote relational misalignment.





#### Qwen2-VL:

This image depicts a vibrant and bustling scene from Times Square in New York City. Buildings and Advertisements:... Notable signs include those for "Coca-Cola," "Disney," and "ABC News."... Traffic and Vehicles:... There are also a few other cars and possibly a bus or two visible in the background. The road has multiple lanes, and there are crosswalks marked on the pavement. Pedestrians: The sidewalks are crowded with people walking and standing. Some pedestrians appear to be tourists, as indicated by their casual attire and the fact that they are taking photos or looking around. Street Elements: There are several potted plants lining the sidewalk...

#### ChatGPT-4o:

The image captures a lively and bustling scene of Times Square in New York City, filled with bright lights, advertisements, and the energy of city life. The street is busy with the iconic yellow taxis driving along clearly marked lanes, accompanied by a few white cars adding to the traffic. A central divider with short bollards helps organize the flow of vehicles, and pedestrian crossings and directional signs are visible on the asphalt, ensuring movement is orderly.

Surrounding the street, towering buildings are adorned with large electronic billboards showcasing advertisements for famous brands, Broadway shows, and various products... Notable advertisements, such as those from Disney and other prominent entertainment companies, add to the commercial appeal of the scene. One of the tallest buildings prominently displays a clock and a digital screen showing promotional content, making it a distinctive feature in the skyline.

#### DeepSeek-VL2:

This image depicts a bustling urban scene, likely in a major city. The image is filled with vibrant colors and a busy street lined with tall buildings. The buildings are adorned with numerous large, brightly lit billboards and advertisements. The advertisements for various products, movies, and brands. The street is filled with yellow taxis, cars, and pedestrians. The street is marked with white lines and has a "NO" sign...

#### LLaVa-1.5:

The image depicts a busy city street filled with traffic, including several cars and taxis. There are multiple cars driving down the street, with some positioned closer to the foreground and others further away. Two taxis are also visible, with one near the center of the scene and another towards the right side. Numerous pedestrians can be seen walking along the sidewalks, with some closer to the foreground and others further back. The street is bustling with activity, and the presence of tall buildings in the background adds to the urban atmosphere.

Object Misalignment      Attribute Misalignment      Relational Misalignment

Figure 5: This figure presents examples of descriptions generated by different LVLMs when given the image shown in the upper left corner. The highlighted text segments in the descriptions represent different types of misalignment. Specifically, red highlights indicate object misalignment. Yellow highlights represent attribute misalignment. Blue highlights denote relational misalignment.



#### ChatGPT-4o:

The image shows a busy classroom filled with students engaging in various creative activities... The chairs are mostly pink, with a few beige ones mixed in, and they are positioned haphazardly around the tables... To the right, another student with blonde hair and a black hoodie is seated, concentrating on a piece of paper with art supplies spread out in front of them. Several black pencil cases are visible on the tables, along with scissors, glue, and other art tools. In the middle of the image, a group of students is gathered around a table... Towards the back of the room, a whiteboard covered with colorful posters, drawings, and notes serves as a focal point... An American flag is displayed in the upper right corner... On the far left, a student wearing a black shirt stands near a ladder, possibly looking for something or observing their classmates. Another student in a pink sweater is seated at a desk, seemingly immersed in their task. In the foreground, bottles of hand sanitizer and cleaning supplies are placed on a table, suggesting an emphasis on hygiene and cleanliness within the classroom.

#### Qwen2-VL:

The image depicts a classroom setting with several students engaged in various activities... Students:... A student in a red shirt is standing near the right side of the room, looking down at something on the floor. Tables:... Some tables have laptops or tablets open, indicating that digital work is being done... Chairs: The chairs are mostly orange and are positioned around the tables... Windows: The room has large windows on the right side, allowing natural light to enter. The windows have blinds, which are partially open. Additional Items: There are several bottles of hand sanitizer placed on the tables... Floor: The floor is carpeted, providing a comfortable environment for the students...

#### DeepSeek-VL2:

The image depicts a classroom setting with multiple students engaged in various activities. All students are seated at tables, working on different tasks. The tables are equipped with chairs. The classroom has shelves filled with supplies. There are posters and papers on the walls. The students are wearing casual clothing. The classroom appears to be well-lit.

#### LLaVa-1.5:

The image depicts a classroom setting with a group of children sitting at tables, working on various projects... The children are engaged in activities such as using laptops, working on papers, and possibly drawing. The room is filled with numerous books scattered across the tables and the floor... In addition to the children and their belongings, there are a few bottles placed around the room, possibly containing drinks for the children. A TV is mounted on the wall, which could be used for presentations or educational purposes.

Object Misalignment      Attribute Misalignment      Relational Misalignment

Figure 6: This figure presents examples of descriptions generated by different LVLMs when given the image shown in the upper left corner. The highlighted text segments in the descriptions represent different types of misalignment. Specifically, red highlights indicate object misalignment. Yellow highlights represent attribute misalignment. Blue highlights denote relational misalignment.